

Accepted Manuscript

Functionalization of nickel nanowires with a fluorophore aiming at new probes for multimodal bioanalysis

Paula C. Pinheiro, Célia T. Sousa, João P. Araújo, António J. Guiomar, Tito Trindade

PII: S0021-9797(13)00728-5
DOI: <http://dx.doi.org/10.1016/j.jcis.2013.07.065>
Reference: YJCIS 19010

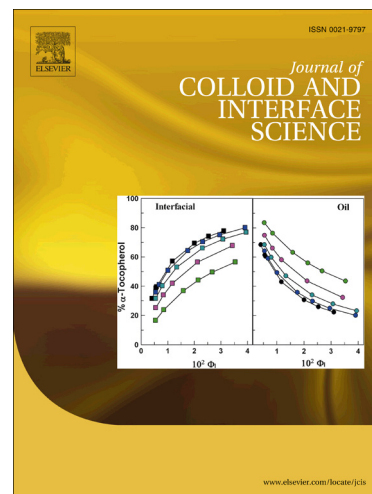
To appear in: *Journal of Colloid and Interface Science*

Received Date: 6 March 2013

Accepted Date: 29 July 2013

Please cite this article as: P.C. Pinheiro, C.T. Sousa, J.P. Araújo, A.J. Guiomar, T. Trindade, Functionalization of nickel nanowires with a fluorophore aiming at new probes for multimodal bioanalysis, *Journal of Colloid and Interface Science* (2013), doi: <http://dx.doi.org/10.1016/j.jcis.2013.07.065>

This is a PDF file of an unedited manuscript that has been accepted for publication. As a service to our customers we are providing this early version of the manuscript. The manuscript will undergo copyediting, typesetting, and review of the resulting proof before it is published in its final form. Please note that during the production process errors may be discovered which could affect the content, and all legal disclaimers that apply to the journal pertain.



Functionalization of nickel nanowires with a fluorophore aiming at new probes for multimodal bioanalysis

Paula C. Pinheiro^a, Célia T. Sousa^b, João P. Araújo^b, António J. Guiomar^c, Tito Trindade^{a*}

^aDepartment of Chemistry-CICECO, Aveiro Institute of Nanotechnology, University of Aveiro, 3810-193 Aveiro, Portugal

^bIFIMUP and IN, Department of Physics, University of Porto, 4169-007 Porto, Portugal

^cDepartment of Life Sciences and CIEPQPF, University of Coimbra, 3001-401 Coimbra, Portugal

*Correspondence at the above address

E-mail: tito@ua.pt

Phone: +351 234 370 726

FAX: +351 234 370 084

Abstract

This work reports research on the development of bimodal magnetic and fluorescent 1D nanoprobes. First, ferromagnetic nickel nanowires (NiNW) have been prepared by Ni electrodeposition in anodic aluminum oxide (AAO) template. The highly ordered self-assembled AAO nanoporous templates were fabricated using a two-step anodization method of aluminum foil. The surface of the NiNW were then modified with polyethyleneimine (PEI) which was previously labeled with an organic dye (fluorescein isothiocyanate: FITC) via covalent bonding. The ensuing functionalized NiNW exhibited the characteristic green fluorescence of FITC and could be magnetically separated from aqueous solutions by using a NdFeB magnet. Finally, the interest of these bimodal NiNW as nanoprobes for *in vitro* cell separation and biolabeling was preliminary assessed in a proof of principle experiment that involved the attachment of biofunctionalized NiNW to blood cells.

Keywords: aluminum oxide template, nickel nanowires, ferromagnetic, surface functionalization, fluorescence, polyethyleneimine.

Introduction

Nanomaterials have unique properties that can be successfully exploited for diverse applications including in the biomedical field [1-4]. Among the broad range of nanomaterials that are currently being investigated for bioapplications, one dimensional (1D) nanostructures have received special attention due to their variable aspect ratio leading to tunable properties [5-7]. In particular, nickel nanowires (NiNW) exhibit ferromagnetic properties that allow easy magnetic manipulation at low external magnetic fields, thus appearing as good candidates for several biomedical applications, including cell manipulation and separation [8-20]. According to reports on comparative studies of magnetic cell separation involving spheroidal nanoparticles and nanowires, the latter systems seem more efficient due to their magnetic anisotropy and strong magnetic moment [8,12,13,17,21,22]. As a result, larger amounts of pure bioanalytes can be isolated using magnetic nanowires. However, the use of NiNW as movable probes to manipulate biological systems has emerged as the distinctive application for these ferromagnetic systems. Indeed, several reports have described the potential use of NiNW as magnetic tweezers for cell manipulation under low-strength magnetic fields. Examples include the possibility to handle cellular and subcellular objects in aqueous environments by rotating magnetic NiNW [23], the controlled manipulation of micro- and nano-scale objects by using mobile microvortices generated by rotating nanowires [24], and the use of such rotating Ni NW for propulsion and cargo transport[25].

Additionally, NiNW can be coupled to other phases in order to extend the chemistry platform offered by these nanostructures. Thus, multisegmented Ni-Au nanowires prepared by template electrodeposition have been used in protein separation from complex biological mixtures, with the Au segment offering additional sites for the chemisorption of S donor molecules [26,27]. The development of NiNW for *in vitro* diagnosis might benefit from the integration of other functionalities that allows complementary uses to magnetic manipulation. In particular, specifically designed fluorescent NiNW can serve as nanoprobe for optical monitoring in magnetic cell manipulation and separation [9,18]. This is particularly relevant as there is evidence that NiNW alone can induce changes in the cytoskeleton [20], hence fluorescent

surface modified NiNW might be an interesting alternative. Although the ferromagnetic properties of NiNW are well established, there is lack of chemical routes that confer fluorescence behaviour to NiNW to be applied as multifunctional nanoprobe [17,28]. Additionally, biofunctionalization strategies aiming the specific interaction of NiNW with biotargets have been scarce.

A common approach to use nanomaterials for biomedical applications is to chemically modify the surface of the nanoparticles to improve their biocompatibility. Polyelectrolytes functionalized with fluorescent entities are convenient systems by which magnetic nanoparticles can be modified to produce fluorescent magnetic carriers [29-34]. In addition, attachment of polyelectrolytes to the NiNW surfaces improves their colloidal stability in aqueous medium. In this work, the attachment of a conventional organic fluorophore (FITC) to the surface of NiNW is reported. It is shown that the polyelectrolyte PEI can act as an effective macromolecular linker to FITC and the NiNW. As a proof of principle experiment, the modified NiNW were employed as fluorescent nanoprobe in the magnetic separation of bovine blood platelets.

Experimental

Chemicals

High purity (> 99.97 %) aluminum foils 250 μm thick and fluorescein isothiocyanate isomer I (FITC, 95 %) were obtained from Alfa Aesar. Branched polyethyleneimine (PEI, $M_w = 25000$), EDTA dipotassium salt dehydrate ($\text{K}_2\text{EDTA} \cdot 2\text{H}_2\text{O}$, $\geq 98\%$), sodium hydroxide (NaOH, $\geq 97\%$), oxalic acid ($\text{H}_2\text{C}_2\text{O}_4$, $\geq 99\%$), ethanol ($\text{C}_2\text{H}_5\text{OH}$, $\geq 99.5\%$), boric acid (H_3BO_3 , $\geq 99.5\%$), nickel (II) sulfate hexahydrate ($\text{NiSO}_4 \cdot 6\text{H}_2\text{O}$, 99 %) and nickel (II) chloride hexahydrate ($\text{NiCl}_2 \cdot 6\text{H}_2\text{O}$, 99.9 %) were purchased from Sigma-Aldrich. The phosphate buffered saline (PBS) used was Dulbecco's PBS, purchased from Invitrogen. All chemicals were used as received and all aqueous solutions were freshly prepared using ultrapure water ($18.2 \text{ m}\Omega \text{ cm}^{-1}$).

Syntheses

Ni nanowires were fabricated by electrodeposition using anodized aluminum oxide (AAO) membrane (Figure 1a) with cylindrical nanopores of 35 nm in diameter and 5 μm thick. These dimensions have been selected in order to obtain high aspect ratio particles whose high coercivity and remanence lead to more efficient cell sorting and bioseparation tasks [35]. Anodization of aluminum foil was carried out by a two-step anodization process with 0.3 M oxalic acid as an anodizing solution at 40 V and 4 °C. Then, nickel was deposited into the pores by electroplating from an acid bath with 350 g/L $\text{NiSO}_4 \cdot 6\text{H}_2\text{O}$, 45 g/L $\text{NiCl}_2 \cdot 6\text{H}_2\text{O}$ and 45 g/L H_3BO_3 at 40 °C and pH 4,5 [36]. Finally, the AAO was dissolved in an aqueous solution of 0.2 M H_2CrO_4 and 0.4 M H_3PO_4 at 60 °C, releasing the NiNW from the membranes. Once in suspension, the wires were collected with a magnet, washed with deionized water and in ethanol.

The synthesis of PEI-FITC was based on the reaction between the isothiocyanate group of FITC and the primary amino group of polyethyleneimine [37]. A reaction scheme for this process is shown in Figure 1b. The FITC (12.6 mg) was added to 312.6 mg PEI in 30 ml ultra-pure water. The resulting solution was kept in dark conditions under magnetic stirring and after adjusting its pH to 11. Dialysis of free FITC was carried out by immersing the dialysis membrane (molecular weight cut-off 12–14 kDa, Medicell International) containing the PEI-FITC solution into 1 L of distilled water, previously placed in a beaker wrapped in aluminum foil, under magnetic stirring and at room temperature. This process took one week, during which the supernatant water has been exchanged daily; the dialysis membrane containing PEI-FITC was kept in dark conditions except during the few minutes required to water exchange.

As illustrated in Figure 1c, the NiNW were then functionalized with PEI-FITC. Hence, 5 mg of the ensuing NiNW were mixed with 5 ml of an aqueous solution of PEI/FITC at pH= 5.5. This mixture was mechanically stirred (600 rpm) at room temperature for 1 h. The resulting functionalized nickel nanowires were collected as powders by using a NdFeB magnet and were thoroughly washed with ultra-pure water.

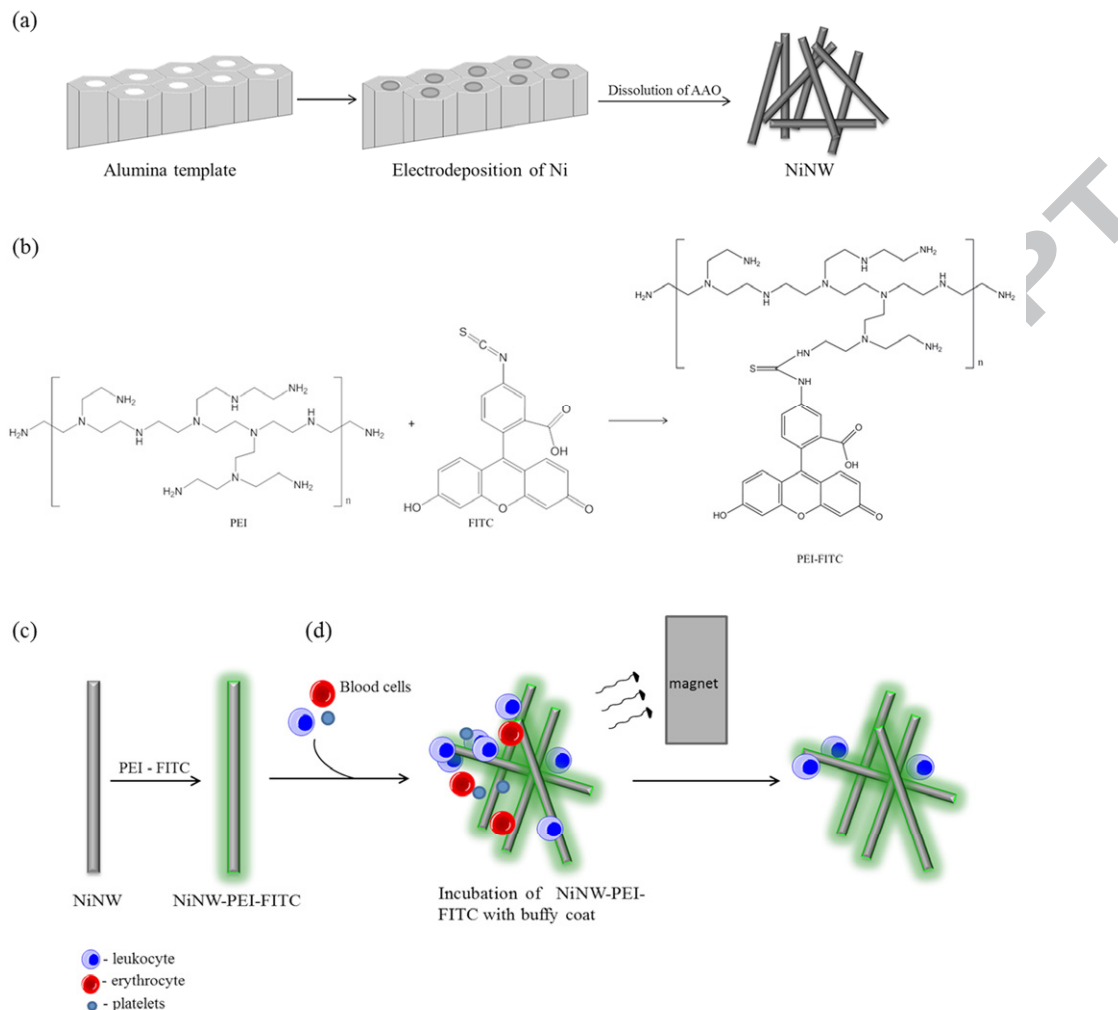


Figure 1- Schemes for the synthesis of NiNW (a); PEI-FITC (b); PEI-FITC coated NiNW (c) and for the cell separation using ferromagnetic NiNW (d). The nanowires were separated using a magnet and washed twice with PBS. Note that the above PEI-FITC structure is one among other possible structures because FITC can form amide bonds with other amine groups of PEI.

Magnetic bioseparation procedure

For *in vitro* cellular interaction experiments, a suspension of bovine blood cells was used. Bovine blood, anticoagulated with K_2EDTA , was fractionated by centrifugation at 1500 g (45 minutes), in order to obtain a leukocyte-rich fraction called buffy coat (located between the upper plasma layer and the lower erythrocyte layer). The collected buffy coat was further centrifuged at 1500 g (10 seconds) in order to reduce the number of erythrocytes present. Functionalized NiNW (1 mg/mL) dispersed in

PBS were added to the cell suspension and rolled for 2 h at room temperature. The Ni nanowires were then separated using a NdFeB magnet and were again resuspended in PBS and washed twice with PBS (Figure 1d). For the fluorescence microscopy studies, 50 μL aliquots of each experiment were placed into the wells of a 8-well μ -Slide (Ibidi, GmbH) and observed with a Zeiss Axiovert 200 inverted fluorescence microscope, using Zeiss Filter Set 02 (excitation: G 365; beam splitter: FT 395; emission: LP 420), allowing excitation near the 365/366 nm mercury line and detection of emission longer than 420 nm.

Characterization of the Ni nanowires

Fourier transform infrared (FTIR) spectra of FITC and PEI-FITC samples were recorded using a spectrometer Bruker optics tensor 27 coupled to a horizontal attenuated total reflectance (ATR) cell, using 256 scans at a resolution of 4 cm^{-1} . The X-ray powder diffraction patterns were recorded using a X-ray diffractometer Philips X'Pert equipped with a $\text{CuK}\alpha$ monochromatic radiation source. Transmission electron microscopy (TEM) analysis was performed by using a FEI Tecnai T20 microscope operating at 200 keV. Samples for TEM analysis were prepared by placing an aliquot of a dilute suspension of Ni NW on a copper grid coated with an amorphous carbon film. For SEM analysis an aliquot of a dilute nanowires suspension was allowed to air dry on glass slides and then were coated with evaporated carbon. SEM was performed using a scanning electron microscope Hitachi SU70 operating at an accelerating voltage of 25 kV. Zeta potential measurements were performed by using a Zetasizer Nanoseries instrument of Malvern Instruments. Fluorescence measurements were performed using a fluorometer FluoroMax3 – HORIBA Jobin Yvon and using quartz cuvettes. The magnetization measurements were performed using a commercial Vibrating Sample Magnetometer (VSM; LOT-Oriel EV7), operating at room temperature, in which an electromagnet provides a magnetic field that reaches the maximum value of 1.5 T (for a minimum gap of 3 cm) and also allows adjustable angles between -180° to 180° during the measurements. The nickel samples employed in the VSM measurements were prepared as follows. The alumina template was first removed as described above. The powders were then thoroughly washed with water and dried under a N_2 stream. Finally the powders were placed in a diamagnetic sample holder where the measurements were carried out.

Results and Discussion

The nickel nanowires (NiNW) used in this research have been fabricated by a template-assisted method, using Ni electrodeposition in anodic aluminum oxide (AAO) templates [38-41]. The morphological characteristics of NiNW prepared by this method can be adjusted by the anodization voltage and time of the second step, during the formation of the membrane in nanoporous AAO [40,41]. The anodizing rate was set at 2.5 $\mu\text{m/h}$ for a deposition time of two hours to produce NiNW with an aspect ratio of 140. The resulting NiNW, after the template removal, were analyzed by vibrating sample magnetometer (VSM) and powder X-ray diffraction (XRD), as well as, by scanning and transmission electron microscopies (SEM and TEM). Figure 2 shows the SEM and TEM images for a typical NiNW sample obtained in these conditions.

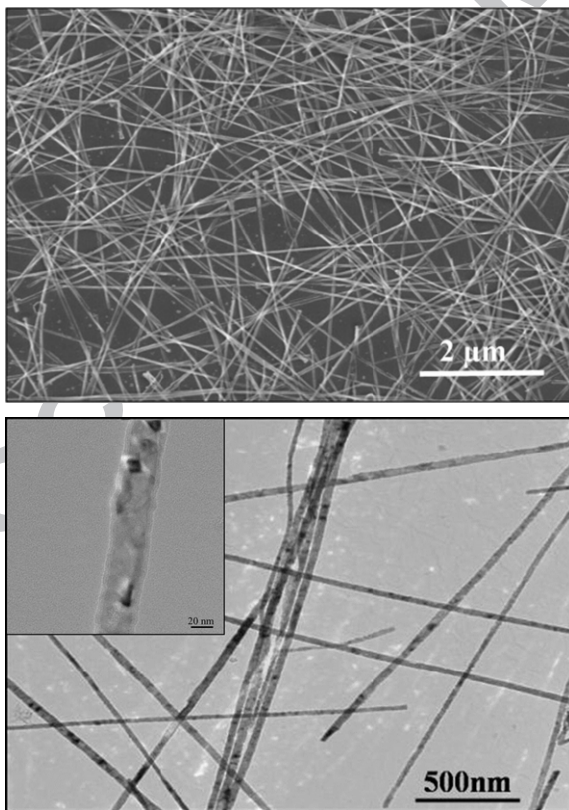


Figure 2- SEM (top) and TEM (bottom) images of nickel nanowires prepared by electrodeposition in alumina template.

The obtained NiNW present homogeneous diameter and length of 35 nm and 5 μm , corresponding to the AAO pore diameter and template thickness, respectively. The powder XRD patterns confirmed unequivocally the presence of the nickel phase (face-centered cubic structure, fcc) exhibiting three peaks that corresponds to the (111), (220) and (200) planes of fcc Ni, with the relative higher intensity of the (111) reflection at $2\theta = 45^\circ$ ascribed to the anisotropic growth of these nanostructures (Figure 3) [21,35,36,42]. As reported by other authors [43,44], the NiNW tend to oxidize at the surface forming a thin oxide layer of NiO (≈ 5 nm) that is usually not detected by XRD due to its amorphous nature. It has been reported that the native metal oxide layer at the surface of the Ni NW limits the cytotoxicity of these materials [23].

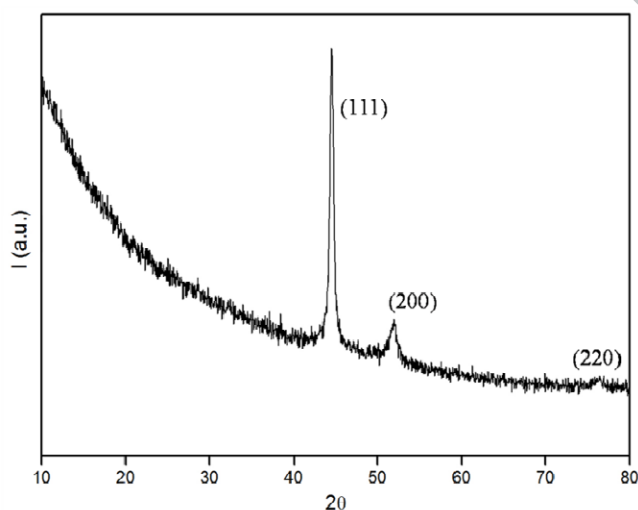


Figure 3- Powder XRD diffraction patterns of nickel nanowires.

The magnetic properties of NiNW have been evaluated by recording the curve of magnetization vs. field $[M(H)]$ ($-15 \leq H \leq 15$ kOe), by using a VSM at room temperature (Figure 4). The $M(H)$ curve shows hysteresis loop with a coercive field (H_c) of 300 Oe indicating that the nanowires are ferromagnetic. The saturation magnetization field was found at 6 KOe, with a saturation magnetic moment of 49.5 emu/g. Arrays of magnetic nanowires present several contributions to the corresponding total magnetic anisotropy. Intrawire and interwire magnetostatic effects

are the dominant features of the anisotropy in packed nanowires. These are the key factors to control the coercive field (H_c) and that influence the magnetization reversal processes [35]. Figure 4 presents the typical hysteresis loop for dispersed Ni NWs after alumina template removal. Out of the template, randomly orientated Ni NWs present a behavior similar to that observed for Ni nanoparticles with a small H_c of 300 Oe and $H_{Sat} = 6$ kOe due to the dipole-dipole interactions (interwire coupling) that overcomes the shape anisotropy, rotating the magnetic easy axis towards an intermediate direction for the nanowires [35].

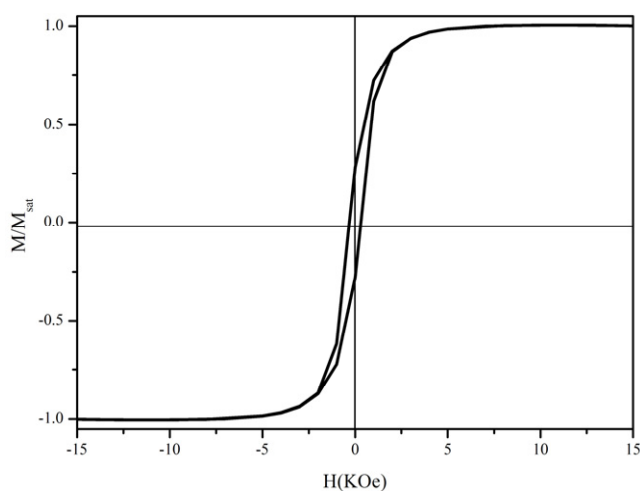


Figure 4- Room temperature $M(H)$ curve for Ni NW powders obtained after alumina template removal and placed onto a diamagnetic sample holder.

Chemical surface modification methods were carried out in order to upgrade the NiNW for fluorescent biolabeling, which together with their intrinsic ferromagnetic characteristics, allows the potential use as multimodal bioprobes. The initial stage along the NiNW surface functionalization involved the grafting of the fluorophore FITC onto the polymer chains of the polyelectrolyte PEI. This has been confirmed by ATR-FTIR spectroscopy, as shown in Figure 5, by comparing the spectrum of PEI-FITC with that one of FITC, the latter shows the characteristic band corresponding to the stretch vibration of the NCS group (2038 cm^{-1}) which is absent in the spectrum of the conjugate. The modification of polyethyleneimine (PEI) with fluorescein isothiocyanate (FITC) involves reaction between the NCS group of FITC with amine group (NHR group) of PEI, resulting in a thiourea bond ($\text{SC}(\text{NR})_2$). Other bands

indicating the presence of FITC are those observed at 1209 cm^{-1} , 1508 cm^{-1} , 1170 cm^{-1} , that can be assigned respectively to C-O-C stretching, C=C stretching, and =C-H bending (Figure 6). The shift of the band at 1618 cm^{-1} in the PEI-FITC spectrum, in relation to the band at 1589 cm^{-1} in the PEI spectrum, may be due to the stretching vibration of C=C bond of FITC. The deviation of the vibrational bands corresponding to the C-N and C-C stretching of PEI, at 1115 cm^{-1} and 1049 cm^{-1} , respectively, to 1026 cm^{-1} and 966 cm^{-1} , is due to proximity of the FITC xanthene ring. In fact, the electronic effects of neighboring groups and hydrogen bonds significantly affect the vibrational modes of a covalent bond [45-47].

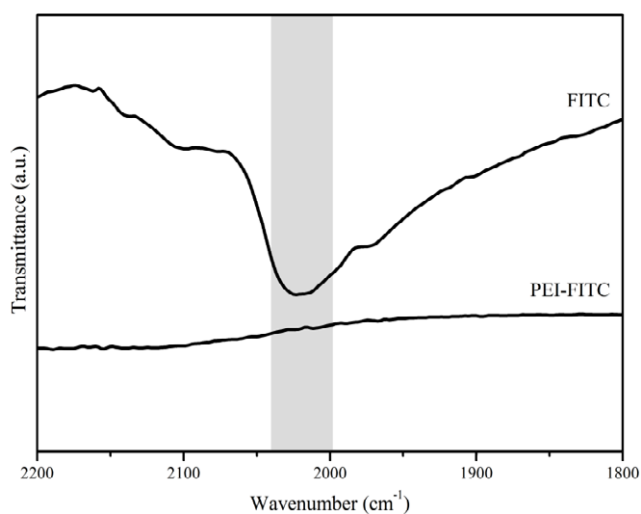


Figure 5- FT-Infrared spectra ($1800\text{-}2200\text{ cm}^{-1}$ region) for the fluorophore FITC and the modified polyelectrolyte PEI-FITC.

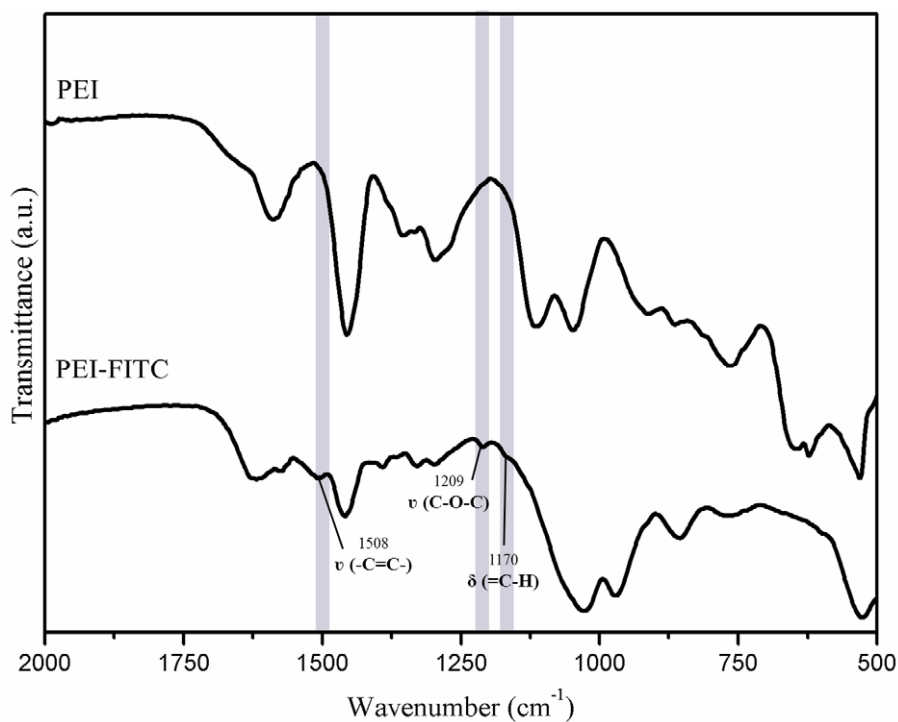


Figure 6- ATR-FTIR of polyelectrolyte PEI and modified polyelectrolyte PEI-FITC.

The functionalized PEI-FITC polyelectrolyte was used to modify the surface of the NiNW. Therefore aqueous suspensions of NiNW were treated with solutions of the functionalized polyelectrolyte and the powders were magnetically separated. In Figure 7, the fluorescence emission spectra of suspensions of these powders exhibit the characteristic absorption due to FITC. We note that these suspensions have been prepared from NiNW that have been magnetically separated and thoroughly washed with distilled water. Hence, the fluorescence observed for the NiNW samples is due to FITC that has been grafted onto the PEI, whose macromolecular chains are interacting with the NiNW surfaces. The bathochromic shift of 16 nm observed in the emission maximum (Figure 7) between PEI-FITC and the fluorophore FITC has previously been reported and is related to the changes of the local environment of dye molecules, such as changes in polarity or polarizability [48,49]. In PEI-FITC, the number of dye molecules that are in each others vicinity increases causing interactions between neighboring molecules, which lowers their excited state energy and produces a red shift in the spectra. These interactions are less favored at the NiNW-PEI-FITC sample

once the polyelectrolyte is adsorbed at the nanowire surface, thus explaining the less pronounced shift observed in the spectrum of the PEI-FITC modified NiNW sample.

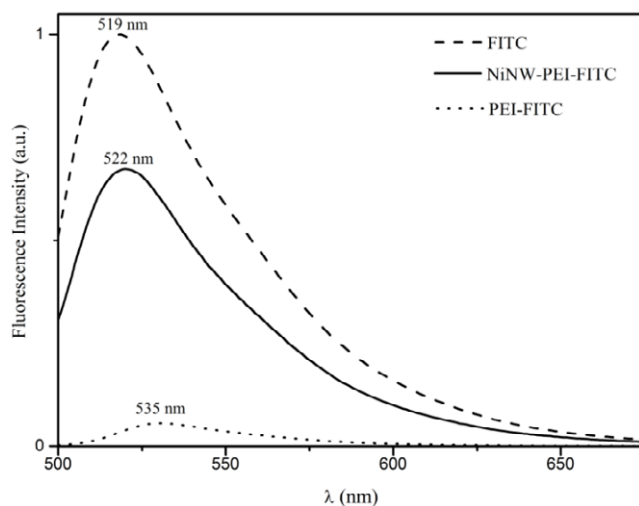


Figure 7- Fluorescence spectra of FITC, PEI conjugated with FITC (PEI-FITC), and functionalized NiNW with PEI-FITC (NiNW-PEI-FITC) (λ_{ex} = 494nm).

Additional evidence for the surface modification of the NiNW was obtained by measuring the zeta potential prior and after treatment with FITC functionalized PEI, a cationic polyelectrolyte. Hence, after surface modification of the nanowires with PEI-FITC a positive zeta potential was obtained (ζ = +49.8 mV, pH 6) as compared to ζ = -33.5 mV, for the non-modified NiNW and at the same pH. The interactions that take place between the polyelectrolyte and the nanowires surface have predominant electrostatic character. However, other types of interactions cannot be excluded, such as hydrogen bonding between surface OH groups (due to nickel oxidation described above) and the amino groups of PEI [50].

Finally, preliminary experiments were carried out as proof of principle for the multifunctionality associated to the modified NiNW as magnetic and fluorescent bioprobes, using a suspension of bovine blood cells. Figure 8 shows the results of optical microscopy applied to the modified NiNW that have contacted the cell suspension and were magnetically separated and washed. The optical transmission image in Figure 8b shows areas containing cells with the morphological characteristics of leukocytes bound to micrometric nanowire aggregates, which indicate close interaction between the cells and the modified NiNW. In fluorescence mode, these areas appear with the typical green fluorescence of FITC (Figure 8c).

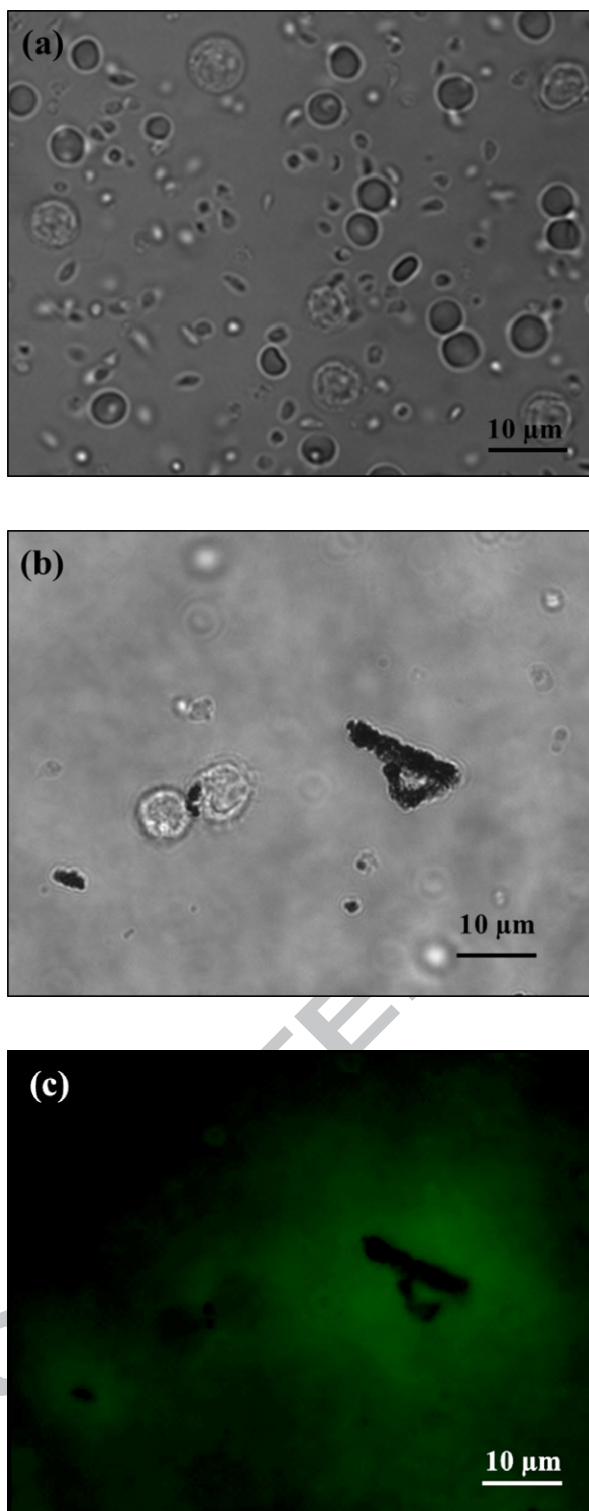


Figure 8- Optical microscopy image of (a) buffy coat showing the three types of blood cells; (b) NiNW/PEI/FITC after contact with buffy coat followed by magnetic separation and washing with PBS (transmission mode); and (c) NiNW/PEI/FITC after contact with buffy coat (fluorescence mode) ($\lambda_{ex}=365$ nm).

Previous studies, which employed leukocyte suspensions, have shown that surface modification with PEI of polyurethane films/filters improved leukocyte removal and adhesion to surfaces; however, no improvement was found when whole blood was used [51,52]. Leukocytes have a negative zeta potential [53] and therefore are prone to interact strongly with the positive surface of the NiNW. However, other types of interactions are certainly involved, such as hydrogen bonding between groups on the leukocyte membrane and electronegative nitrogen atoms of PEI [52-54]. Moreover, it has been widely accepted that surface wettability and hydrophilicity also influence the adhesion of leukocytes [53,54]. As such, the mechanism of the cell-PEI-NiNW interaction cannot be anticipated at this stage.

Leukocyte adhesion plays a predominant role in leukocyte depletion, which is applied clinically to remove these cells from blood. In some situations, such as in blood transfusion, it is necessary to reduce the concentration of leukocytes in blood, in order to prevent leukocyte-mediated adverse effects [51,54,55]. Therefore, the materials described here may contribute to develop additional tools for the depletion of leukocytes, taking advantage of the ferromagnetic properties of nickel nanowires.

Conclusions

In conclusion, ferromagnetic nickel nanowires prepared on anodic aluminum oxide template have been surface modified with polyethyleneimine with minimal effects on their magnetic separation from aqueous solutions. An improvement on this surface modification strategy comprises the functionalization of the polyelectrolyte with fluorescein isothiocyanate. In this way, not only the NiNW can be used as ferromagnetic nanodrivers or nanotweezers for magnetic biomanipulation procedures, but optical labeling is also possible due to the green fluorescence typical of the organic dye. Although a detailed study on the interaction of the modified NiNW with the blood cells in variable conditions was out of the scope of this research, these results suggest that these materials might be useful in magnetic separation/manipulation and fluorescent labeling of leukocytes, for which the functionalized NiNWs seem to have stronger affinity. However, the use of these systems has yet to be established in real *in vitro* bioanalysis by evaluating the diverse

variables that could affect their performance. This aspect has great relevance namely due to the possibility of interactions between the NiNW surfaces and other blood cells. Future research on these fluorescent ferromagnetic NiNW might bring further evidence for their potential use in magnetic manipulation of blood cells by taking into account specific biorecognition issues.

Acknowledgements

We thank Fundação para a Ciência e Tecnologia (NANO/NMed-SD/0140/2007, ERA-Eula/0003/2009 and Pest-C/CTM/LA0011/2011), FSE and POPH for funding. We also thank Luísa Cortes (Center for Neurosciences and Cell Biology, Coimbra, Portugal) for valuable technical assistance with the microscope. Célia T. Sousa is also thankful to FCT for post-doctoral grant SFRH/BPD/82010/2011.

References

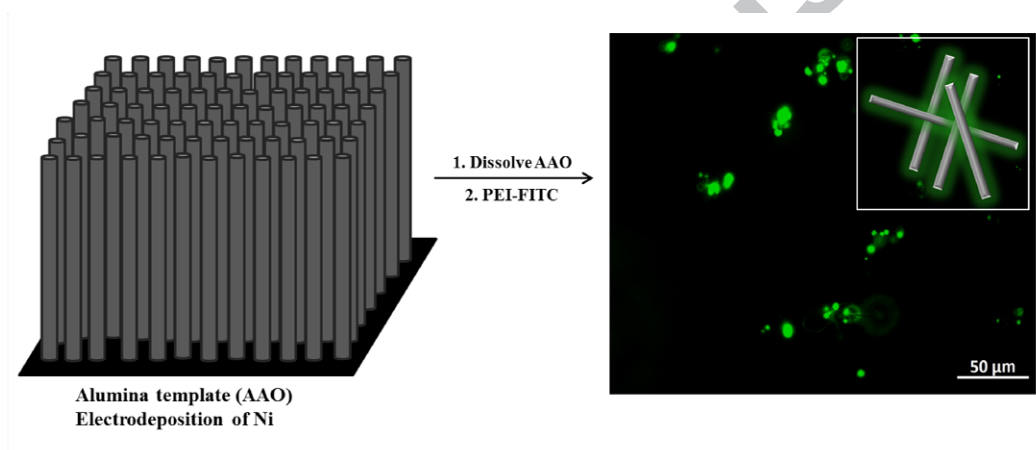
- [1] T. Trindade, A. L. Daniel-da-Silva, *Nanocomposite Particles for Bio-Applications – Materials and Bio-Interfaces*, Pan Stanford Publishing: Singapore, 2011.
- [2] G. A. Ozin, A. C. Arsenault, L. Cademartiri, *Nanochemistry: A Chemical Approach to nanomaterials*; Royal Society of Chemistry: Toronto, 2005.
- [3] S. H. Lee, J. H. Sung, T. H. Park, *Ann. Biomed. Eng.*, 40 (2012) 1384.
- [4] Q. A. Pankhurst, J. Connolly, S. K. Jones, J. Dobson, *J. Phys. D.: Appl. Phys.*, 36 (2003) R167.
- [5] N. Chopra, V. G. Gavalas, B. J. Hinds, L. G. Bachas, *Anal. Lett.*, 40 (2007) 2067.
- [6] C. D. Keating, M. Natan, *Adv. Mater.*, 15 (2003) 451.
- [7] J. Wang, *ChemPhysChem*, 10 (2009) 1748.
- [8] M. Vazquez, K. Pirola, M. Hernandez-Velez, V. M. Prida, D. Navas, R. Sanz, F. Batallan, J. Velazquez, *J. Appl. Phys.*, 95 (2004) 6642.
- [9] A. Prina-Mello, Z. Diao, J. M. D. Coey, *J. Nanobiotechnology*, 4 (2006) 1.
- [10] M. Tanase, E. J. Felton, D. S. Gray, A. Hultgren, C. S. Chen, D. H. Reich, *Lab Chip*, 5 (2005) 598.
- [11] D. Choi, A. Fung, H. Moon, D. Ho, Y. Chen, E. Kan, Y. Rheem, B. Yoo, N. Myung, *Biomed. Microdevices*, 9 (2007) 143.
- [12] N. Gao, X. Yang, Y. T. Tsai, G. M. Chu, H. Wang, E. H. Yang, *Proc. of SPIE*, 7318 (2009) 73181E-1.
- [13] A. Hultgren, M. Tanase, C. S. Chen, G. J. Meyer, D. H. Reich, *J. Appl. Phys.*, 93 (2003) 7554.
- [14] A. Hultgren, M. Tanase, C. S. Chen, D. H. Reich, *IEEE Tran. Magnetics*, 40 (2004) 2988.

- [15] D. H. Reich, M. Tanase, A. Hultgren, L. A. Bauer, C. S. Chen, G. J. Meyer, J. Appl. Phys., 93 (2003) 7275.
- [16] L. A. Bauer, N. S. Birenbaum, G. J. Meyer, J. Mater. Chem., 14 (2004) 517.
- [17] A. Hultgren, M. Tanase, E. J. Felton, K. Bhadriraju, A. K. Salem, C. S. Chen, D. H. Reich, Biotechnol. Prog., 21 (2005) 509.
- [18] A. O. Fung, V. Kapadia, E. Pierstorff, D. Ho, Y. J. Chen, Phys. Chem. C, 112 (2008) 15085.
- [19] N. Gao, H. Wang, E. H. Yang, Nanotechnology, 21 (2010) 1.
- [20] F. Johansson, M. Jonsson, K. Alm, M. Kanje, Exp. Cell Res., 316 (2010) 688.
- [21] F. Byrne, A. Prina-Mello, A. Whelan, B. Mohamed, A. Davies, Y. Gunko, J. M. D. Coey, Y. Volkov, J. Magn. Magn. Mater., 321 (2009) 1341.
- [22] A. A. Wang, J. Lee, G. Jenikova, A. Mulchandani, N. V. Myung, W. Chen, Nanotechnology, 17 (2006) 3375.
- [23] L. Zhang, T. Petit, K. E. Peyer, B. J. Nelson, Nanomedicine, 7 (2012) 1074.
- [24] T. Petit, L. Zhang, K. E. Peyer, B. E. Kratochvil, B. J. Nelson, Nano Lett., 12 (2012) 156.
- [25] L. Zhang, T. Petit, Y. Lu, B. E. Kratochvil, K. E. Peyer, R. Pei, J. Lou, B. J. Nelson, ACS Nano, 4 (2010) 6228.
- [26] K. B. Lee, S. Park, C. A. Mirkin, Angew. Chem. Int., 43 (2004) 3048.
- [27] N. S. Birenbaum, B. T. Lai, C. S. Chen, D. H. Reich, G. J. Meyer, Langmuir, 19 (2003) 95802.
- [28] C. L. Chien, L. Sunb, M. Tanasea, L. A. Bauerc, A. Hultgrena, D. M. Silevitcha, G. J. Meyerc, P. C. Searsonb, D. H. Reich, J. Magn. Magn. Mater., 249 (2002) 146.
- [29] C. Kaewsaneha, P. Opaprakasit, D. Polpanich, S. Smanmoo, P. Tangboriboonrat, J. Coll. Interf. Sci., 377 (2012) 145.

- [30] W. Xu, J. Y. Park, K. Kattel, M. W. Ahmad, B. A. Bony, W. C. Heo, S. Jin, J. W. Park, Y. Chang, T. J. Kim, J. A. Park, J. Y. Do, K. S. Chae, G. H. L. Lee, *RSC Adv.*, 2 (2012) 10907.
- [31] Y. Okamoto, F. Kitagawa, K. Otsuka, *Anal. Chem.*, 79 (2007) 3041.
- [32] Y. Ge, Y. Zhang, S. He, F. Nie, G. Teng, N. Gu, *Nanoscale Res. Lett.*, 4 (2009) 287.
- [33] P. Govindaiah, T. Hwang, H. Yoo, Y. S. Kim, S. J. Lee, S. W. Choi, J. H. Kim, *J. Coll. Interf. Sci.*, 379 (2012) 27.
- [34] X. Hong, J. Li, M. Wang, J. Xu, W. Guo, J. Li, Y. Bai, T. Li, *Chem. Mater.*, 16 (2004) 4022.
- [35] M. Vazquez, K. Pirota, J. Torrejon, D. Navas, M. Hernandez-Velez, *J. Magn. Mater.*, 294 (2005) 174.
- [36] M. P. Proença, C.T. Sousa, J. Ventura, M. Vazquez, J.P. Araújo, *Electrochim. Acta*, 72 (2012) 215.
- [37] G. T. Hermanson, *Bioconjugate Techniques*; Academic Press: London, 1996.
- [38] M. Lai, D. J. Riley, *J. Coll. Interf. Sci.*, 323 (2008) 203.
- [39] J. P. O'Sullivan, G. C. Wood, *Proc. R. Soc. Mater.*, 128 (2000) 582.
- [40] C. T. Sousa, D. C. Leitão, M. P. Proença, A. Apolinário, J. G. Correia, J. Ventura, J. P. Araújo, *Nanotechnology*, 22 (2011) 1.
- [41] W. Lee, R. Ji, U. Gosele, K. Nielsch, *Nature Mater.*, 9 (2006) 741.
- [42] G. B. Cheng, G. C. Wei, C. J. Hao, S. T. Li, *Electron. Mater. Lett.*, 5 (2009) 123.
- [43] Z. F. Zhou, Y. C. Zhou, Y. Pan, W. X. Lei, C. F. Xu, *Scr. Mater.*, 60 (2009) 512.
- [44] L. He, Z. M. Liao, H. C. Wu, X. X. Tian, D. S. Xu, G. L. W. Cross, G. S. Duesberg, I. V. Shvets, D. P. Yu, *Nano Lett.*, 11 (2011) 4601.

- [45] A. Lex, P. Pacher, O. Werzer, A. Track, Q. Shen, R. Schennach, G. Koller, G. Hlawacek, E. Zojer, R. Resel, M. Ramsey, C. Teichert, W. Kern, G. Trimmel, *Chem. Mater.*, 20 (2008) 2009.
- [46] B. H. Stuart, *Infrared Spectroscopy: Fundamentals and applications*. Wiley: New York, 2004.
- [47] L. P. Donald, M. L. Gary, S. K. George, R. V. James, *Introduction to spectroscopy*. Brooks/Cole: California, 2009.
- [48] E. W. Voss Jr., J. C. Croney, D. M. Jameson, *J. Protein Chem.*, 21 (2002) 231.
- [49] A. Imhof, M. Megens, J. J. Engelberts, D. T. N. Lang, R. Sprik, W. L. Voss, *J. Phys. Chem. B*, 103 (1999) 1408.
- [50] J. Gregory, S. Barany, *Adv. Colloid Interface Sci.*, 169 (2011) 1.
- [51] A. Bruil, H. A. Oosterom, I. Steneker, B. J. M. Al, T. Beugeling, W. G. Aken, J. Feijen, *J. Biomed. Mater. Res.*, 27 (1993) 1253.
- [52] A. Bruil, J. G. A. Terlingen, T. Beugeling, W. G. Aken, J. Feijen, *Biomaterials*, 13 (1992), 915.
- [53] M. M. B. Ribeiro, M. M. Domingues, J. M. Freire, N. C. Santos, M. A. R. B. Castanho, *Front. Cell. Neurosci.*, 6 (2012) 1.
- [54] A. Bruil, T. Beugeling, J. Feijen, W. G. Aken, *Transfus. Med. Rev.*, 9 (1995) 145.
- [55] S. Singh, A. Kumar, *Biotechnol. J.*, 4 (2009) 1140.

Graphical abstract



Highlights

- Nickel electrodeposition in anodic aluminum oxide template forming nanowires.
- Functionalization of polyethyleneimine with a fluorophore (FITC)
- Ferromagnetic nanowires functionalized with FITC- grafted polyethyleneimine.
- New bimodal magnetic/fluorescent nanoprobe for *in vitro* experiments.